

# Continuity-Enhanced Basis Signal aided Low-Interference $N$ -Continuous OFDM

Peng Wei, Yue Xiao, Lilin Dan

**Abstract**—A novel linear combination representation aided time-domain smooth signal design is proposed by continuity-enhanced basis signals for the  $N$ -continuous orthogonal frequency division multiplexing (NC-OFDM) system. Compared to the conventional NC-OFDM, the proposed scheme is capable of reducing the interference and maintaining the same sidelobe suppression performance imposed with the aid of two groups of basis signals assisted by the linear combination form. Our performance results demonstrate that with a low complexity overhead, the proposed scheme is capable of improving the error performance in comparison to the conventional NC-OFDM, while maintaining the same sidelobe suppression as the conventional counterpart.

**Index Terms**—Interference,  $N$ -continuous orthogonal frequency division multiplexing (NC-OFDM), sidelobe suppression.

## I. INTRODUCTION

SINCE the invention of  $N$ -continuous orthogonal frequency division multiplexing (NC-OFDM) by Beek *et al.* [1], [2], sidelobe suppression based on the  $N$ -continuity criterion in which the signal is made continuous up to the  $N$ th-order derivative has been developed in the context of a class of frequency-domain precoders [1]–[7]. Although the  $N$ -continuity criterion has been widely employed for suppressing sidelobes, precoding in frequency domain does not necessarily guarantee the direct elimination of the self-interference in the multipath fading channel. For example, the self-interference caused by precoders in [1], [2] increases the signal-to-noise ratio (SNR) loss, selected mapping (SLM) in [3] and cancellation tones in [4] are capable of reassigning the interference which can be reduced at the price of high complexity. By contrast, the family of self-interference reduction precoders [8], [9] was designed to directly reduce the self-interference by only adding the precoder-induced interference in the guard interval, which is composed of a prefix or both prefix and suffix, and hence, it was shown to outperform other precoding solutions in the general performance associated with sidelobe suppression, complexity, and bit error ratio (BER). However, the interference added in the whole guard interval increases the sensitivity to channel-induced intersymbol interference (ISI) and intercarrier interference (ICI) as analyzed in [9]. Moreover, the precoder in [8] needs the data of the previous symbol to construct the  $N$ -continuous signal which means extra memory consumption. In recent years, studies

of time-domain signal format have found reduced-complexity applications in wireless communication systems [10], [11]. More specifically, the linear combination-based  $N$ -continuous transmitter was designed with the aid of basis signals.

Against this background, the novel contribution of this letter is that two linear-combination representations aided time-domain  $N$ -continuous OFDM scheme is proposed upon improving continuities of basis signals, for the sake of adaptively controlling the self-interference without degrading its sidelobe suppression performance compared to conventional NC-OFDM.

## II. SYSTEM ASPECT

In a baseband OFDM system, the input bit stream of the  $i$ th OFDM symbol is first modulated onto an uncorrelated complex-valued data vector  $\mathbf{d}_i = [d_{i,k_0}, d_{i,k_1}, \dots, d_{i,k_{K-1}}]^T$  drawn from a constellation, such as phase-shift keying (PSK) or quadrature amplitude modulation (QAM). The complex-valued data vector is mapped onto  $K$  subcarriers with the index set  $\mathcal{K} = \{k_0, k_1, \dots, k_{K-1}\}$ . An OFDM signal is formed by summing all the  $K$ -modulated orthogonal subcarriers with equal frequency spacing  $\Delta f = 1/T_s$ , where  $T_s$  is the OFDM symbol duration. After the OFDM signal is oversampled by a time-domain sampling interval  $T_{\text{samp}} = T_s/M$ , the discrete-time OFDM signal is expressed as

$$x_i(m) = \frac{1}{M} \sum_{r=0}^{K-1} d_{i,k_r} e^{j2\pi \frac{k_r}{M} m}, \quad (1)$$

where  $m \in \mathcal{M} \triangleq \{-M_{\text{cp}}, \dots, 0, \dots, M-1\}$  and  $M_{\text{cp}}$  is the length of cyclic prefix (CP).

## III. LOW-INTERFERENCE TIME-DOMAIN NC-OFDM

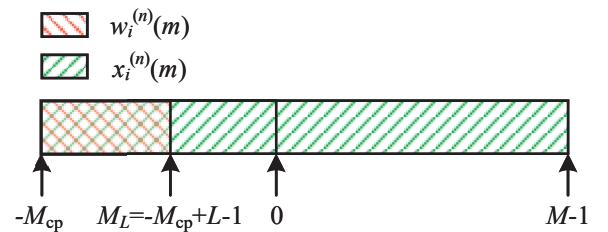


Fig. 1. Illustration of the two discontinuities of the derivatives of the low-interference  $N$ -continuous signal in a baseband-equivalent OFDM symbol.

As shown in Fig. 1, by aligning the beginning of the smooth signal  $w_i(m)$  with that of the CP-appended OFDM symbol  $x_i(m)$ , the smooth signal  $w_i(m)$  is directly added to

P. Wei is with the School of Electronics and Information Engineering, Tianjin Polytechnic University, Tianjin, China (e-mail: wpwwhttp@163.com).

L. Dan and Y. Xiao are with the National Key Laboratory of Science and Technology on Communications, University of Electronic Science and Technology of China, Chengdu, China (e-mail: {lilindan, xiaoyue}@uestc.edu.cn).

the OFDM signal  $x_i(m)$ , and hence, the low-interference  $N$ -continuous OFDM signal  $\bar{x}_i(m)$  is expressed as

$$\bar{x}_i(m) = x_i(m) + w_i(m). \quad (2)$$

Since the length of  $w_i(m)$  is smaller than that of  $x_i(m)$ , to generate the  $N$ -continuous signal, two discontinuities are required to be smoothed. As depicted in Fig. 1, the first one at the point  $-M_{cp}$  is caused by  $x_i(m)$  and the second one at the point  $M_L = -M_{cp} + L - 1$  is introduced by  $w_i(m)$  with the support length of  $L$ , which are, respectively, corresponding to the beginning and the end of  $w_i(m)$ .

Thus, to meet  $N$ -continuity criterion at the point  $-M_{cp}$ ,  $w_i(m)$  should satisfy

$$w_i^{(n)}(m) \Big|_{m=-M_{cp}} = x_{i-1}^{(n)}(m) \Big|_{m=M} - x_i^{(n)}(m) \Big|_{m=-M_{cp}}, \quad (3)$$

where  $n \in \mathcal{U}_N = \{0, 1, \dots, N\}$  with the highest derivative order (HDO)  $N$  and  $x_i^{(n)}(m)$  represents the  $n$ th derivative of  $x_i(m)$ . At the same time, when the  $w_i(m)$  and its first  $N_1$  derivatives are continuous at the point  $M_L$  for  $N_1 = 1, 2, \dots, N$ ,  $w_i(m)$  at the point  $M_L$  should satisfy

$$w_i^{(n)}(m) \Big|_{m=M_L} = 0, \quad n = N_1 + 1, \dots, N. \quad (4)$$

To obtain the  $w_i(m)$  satisfying (3) and (4), two linear combinations composed of two basis signals are formulated as

$$w_i(m) = \begin{cases} \sum_{n=0}^N b_{i,n} f_n(m) + \sum_{n=0}^{N-N_1-1} \tilde{b}_{i,n} \tilde{f}_n(m), & m \in \mathcal{L}, \\ 0, & m \in \mathcal{M} \setminus \mathcal{L}, \end{cases} \quad (5)$$

where  $\mathcal{L} \triangleq \{-M_{cp}, -M_{cp} + 1, \dots, M_L\}$  indicates the range of  $w_i(m)$  implying that the self-interference caused by  $w_i(m)$  can be adaptively adjusted by  $L$ , and more importantly, to satisfy the condition in (4), the continuity-enhanced basis signals  $f_n(m)$  and  $\tilde{f}_n(m)$  are, respectively, designed as

$$f_n(m) = g_n(m) s_1(m) u(m + M_{cp}), \quad (6)$$

$$\tilde{f}_n(m) = \tilde{g}_n(m) s_2(m) u(-m + |M_L|), \quad (7)$$

which, respectively, belong to basis sets  $\mathcal{Q}$  and  $\tilde{\mathcal{Q}}$ , defined as

$$\mathcal{Q} \triangleq \left\{ \mathbf{q}_n \mid \mathbf{q}_n = [f_n(-M_{cp}), f_n(-M_{cp}+1), \dots, f_n(M_L)]^T, \right. \\ \left. n \in \mathcal{U}_N \right\}, \quad (8)$$

$$\tilde{\mathcal{Q}} \triangleq \left\{ \tilde{\mathbf{q}}_n \mid \tilde{\mathbf{q}}_n = [\tilde{f}_n(-M_{cp}), \tilde{f}_n(-M_{cp}+1), \dots, \tilde{f}_n(M_L)]^T, \right. \\ \left. n \in \mathcal{U}_N \right\}. \quad (9)$$

Similar to [9], [10],  $g_n(m)$  and  $\tilde{g}_n(m)$  are calculated by

$$g_n(m) = \frac{1}{M} \left( j \frac{2\pi}{M} \right)^n \sum_{k_r \in \mathcal{K}} k_r^n e^{j2\pi \frac{k_r}{M} (m + M_{cp})}, \quad (10)$$

$$\tilde{g}_n(m) = \frac{1}{M} \left( j \frac{2\pi}{M} \right)^n \sum_{k_r \in \mathcal{K}} k_r^n e^{j2\pi \frac{k_r}{M} (m + M_{cp} - L)}, \quad (11)$$

$s_1(m)$  and  $s_2(m)$  are the truncation windows for improving the continuities of  $w_i(m)$  and its higher-order derivatives satisfying (4), and  $u(m)$  is the unit step function. Using the Blackman window  $s(m) = 0.42 - 0.5 \cos(\frac{\pi m}{L-1}) + 0.08 \cos(\frac{2\pi m}{L-1})$  as the truncation window yields

$$s_1(m) = s(m + M_{cp} + L - 1), \quad (12)$$

$$s_2(m) = s(m + M_{cp}). \quad (13)$$

Then, based on the given  $f_n(m)$  and  $\tilde{f}_n(m)$ , the coefficients  $b_{i,n}$  and  $\tilde{b}_{i,n}$  will be calculated to generate the  $w_i(m)$  as follows. Firstly, Eq. (5) is rewritten in the matrix form as

$$\mathbf{w}_i = \mathbf{Q}_f \mathbf{b}_i + \mathbf{Q}_{\tilde{f}} \tilde{\mathbf{b}}_i, \quad (14)$$

where  $\mathbf{Q}_f = [\mathbf{q}_0 \ \mathbf{q}_1 \ \dots \ \mathbf{q}_N]$  and  $\mathbf{b}_i = [b_{i,0}, b_{i,1}, \dots, b_{i,N}]^T$ . Since the Blackman window and its first derivative are continuous, that is  $N_1 = 1$ , we have  $\mathbf{Q}_{\tilde{f}} = [\tilde{\mathbf{q}}_0 \ \tilde{\mathbf{q}}_1 \ \dots \ \tilde{\mathbf{q}}_{N-2}]$  and  $\tilde{\mathbf{b}}_i = [\tilde{b}_{i,0}, \tilde{b}_{i,1}, \dots, \tilde{b}_{i,N-2}]^T$ . Secondly, substituting (14) into (3) and (4) yields

$$\begin{bmatrix} \mathbf{P}_f & \mathbf{P}_{\tilde{f}} \\ \mathbf{P}_{f_L} & \mathbf{P}_{\tilde{f}_L} \end{bmatrix} \begin{bmatrix} \mathbf{b}_i \\ \tilde{\mathbf{b}}_i \end{bmatrix} = \begin{bmatrix} \Delta \mathbf{x}_i \\ \mathbf{0}_{(N+1) \times 1} \end{bmatrix}, \quad (15)$$

where the matrices  $\mathbf{P}_f$ ,  $\mathbf{P}_{\tilde{f}}$ ,  $\mathbf{P}_{f_L}$ , and  $\mathbf{P}_{\tilde{f}_L}$  are, respectively, expressed as

$$\mathbf{P}_f = \begin{bmatrix} f_0(-M_{cp}) & f_1(-M_{cp}) & \dots & f_N(-M_{cp}) \\ f_0^{(1)}(-M_{cp}) & f_1^{(1)}(-M_{cp}) & \dots & f_N^{(1)}(-M_{cp}) \\ \vdots & \vdots & \ddots & \vdots \\ f_0^{(N)}(-M_{cp}) & f_1^{(N)}(-M_{cp}) & \dots & f_N^{(N)}(-M_{cp}) \end{bmatrix},$$

$$\mathbf{P}_{\tilde{f}} = \begin{bmatrix} 0 & 0 & \dots & 0 \\ 0 & 0 & \dots & 0 \\ \tilde{f}_0^{(2)}(-M_{cp}) & \tilde{f}_1^{(2)}(-M_{cp}) & \dots & \tilde{f}_{N-2}^{(2)}(-M_{cp}) \\ \vdots & \vdots & \ddots & \vdots \\ \tilde{f}_0^{(N)}(-M_{cp}) & \tilde{f}_1^{(N)}(-M_{cp}) & \dots & \tilde{f}_{N-2}^{(N)}(-M_{cp}) \end{bmatrix},$$

$$\mathbf{P}_{f_L} = \begin{bmatrix} 0 & 0 & \dots & 0 \\ 0 & 0 & \dots & 0 \\ f_0^{(2)}(M_L) & f_1^{(2)}(M_L) & \dots & f_N^{(2)}(M_L) \\ \vdots & \vdots & \ddots & \vdots \\ f_0^{(N)}(M_L) & f_1^{(N)}(M_L) & \dots & f_N^{(N)}(M_L) \end{bmatrix},$$

$$\mathbf{P}_{\tilde{f}_L} = \begin{bmatrix} \tilde{f}_0(M_L) & \tilde{f}_1(M_L) & \dots & \tilde{f}_{N-2}(M_L) \\ \tilde{f}_0^{(1)}(M_L) & \tilde{f}_1^{(1)}(M_L) & \dots & \tilde{f}_{N-2}^{(1)}(M_L) \\ \vdots & \vdots & \ddots & \vdots \\ \tilde{f}_0^{(N)}(M_L) & \tilde{f}_1^{(N)}(M_L) & \dots & \tilde{f}_{N-2}^{(N)}(M_L) \end{bmatrix},$$

and  $\Delta \mathbf{x}_i$  is an  $(N+1) \times 1$  vector of the differences between  $\mathbf{x}_i$  and  $\mathbf{x}_{i-1}$ , as well as their first  $N$  derivatives at the point  $-M_{cp}$ , which can be calculated by

$$\Delta \mathbf{x}_i = \mathbf{P}_1 \mathbf{d}_{i-1} - \mathbf{P}_2 \mathbf{d}_i, \quad (16)$$

where

$$\mathbf{P}_1 = \frac{1}{M} \begin{bmatrix} 1 & 1 & \dots & 1 \\ \frac{j2\pi k_0}{M} & \frac{j2\pi k_1}{M} & \dots & \frac{j2\pi k_{K-1}}{M} \\ \vdots & \vdots & \ddots & \vdots \\ \left( \frac{j2\pi k_0}{M} \right)^N & \left( \frac{j2\pi k_1}{M} \right)^N & \dots & \left( \frac{j2\pi k_{K-1}}{M} \right)^N \end{bmatrix},$$

$$\bar{\mathbf{x}}_i = \begin{cases} \mathbf{x}_i + \begin{bmatrix} [\mathbf{Q}_f & \mathbf{Q}_{\tilde{f}}] \begin{bmatrix} \mathbf{P}_f & \mathbf{P}_{\tilde{f}} \\ \mathbf{P}_{f_L} & \mathbf{P}_{\tilde{f}_L} \end{bmatrix}^{-1} \begin{bmatrix} \mathbf{P}_1 \mathbf{d}_{i-1} - \mathbf{P}_2 \mathbf{d}_i \\ \mathbf{0}_{(N+1) \times 1} \end{bmatrix} \\ \mathbf{0}_{(M+M_{cp}-L) \times 1} \end{bmatrix}, & 0 \leq i \leq M_s - 1, \\ [\mathbf{Q}_f & \mathbf{Q}_{\tilde{f}}] \begin{bmatrix} \mathbf{P}_f & \mathbf{P}_{\tilde{f}} \\ \mathbf{P}_{f_L} & \mathbf{P}_{\tilde{f}_L} \end{bmatrix}^{-1} \begin{bmatrix} \mathbf{P}_1 \mathbf{d}_{i-1} - \mathbf{P}_2 \mathbf{d}_i \\ \mathbf{0}_{(N+1) \times 1} \end{bmatrix}, & i = M_s, \end{cases} \quad (20)$$

$\mathbf{P}_2 = \mathbf{P}_1 \Phi$ ,  $\Phi \triangleq \text{diag}(e^{j\varphi k_0}, e^{j\varphi k_1}, \dots, e^{j\varphi k_{K-1}})$ , and  $\varphi = -2\pi M_{cp}/M$ . Lastly, when the rank of the coefficient matrix  $\begin{bmatrix} \mathbf{P}_f & \mathbf{P}_{\tilde{f}} \\ \mathbf{P}_{f_L} & \mathbf{P}_{\tilde{f}_L} \end{bmatrix}$  equals to that of the augmented matrix  $\begin{bmatrix} \mathbf{P}_f & \mathbf{P}_{\tilde{f}} & \Delta \mathbf{x}_i \\ \mathbf{P}_{f_L} & \mathbf{P}_{\tilde{f}_L} & \mathbf{0}_{(N+1) \times 1} \end{bmatrix}$  in (15), according to (15) and (16), the coefficients can be expressed by

$$\begin{bmatrix} \mathbf{b}_i \\ \tilde{\mathbf{b}}_i \end{bmatrix} = \begin{bmatrix} \mathbf{P}_f & \mathbf{P}_{\tilde{f}} \\ \mathbf{P}_{f_L} & \mathbf{P}_{\tilde{f}_L} \end{bmatrix}^{-1} \begin{bmatrix} \mathbf{P}_1 \mathbf{d}_{i-1} - \mathbf{P}_2 \mathbf{d}_i \\ \mathbf{0}_{(N+1) \times 1} \end{bmatrix}. \quad (17)$$

Furthermore, if the inverse of matrix  $\mathbf{P}_f - \mathbf{P}_{\tilde{f}} \mathbf{P}_{\tilde{f}_L}^{-1} \mathbf{P}_{f_L}$  (or  $\mathbf{P}_{\tilde{f}_L} - \mathbf{P}_{f_L} \mathbf{P}_f^{-1} \mathbf{P}_{\tilde{f}}$ ) exists, Eq. (17) can also be expressed as

$$\mathbf{b}_i = (\mathbf{P}_f - \mathbf{P}_{\tilde{f}} \mathbf{P}_{\tilde{f}_L}^{-1} \mathbf{P}_{f_L})^{-1} \Delta \mathbf{x}_i, \quad (18a)$$

$$\tilde{\mathbf{b}}_i = -\mathbf{P}_{\tilde{f}_L}^{-1} \mathbf{P}_{f_L} (\mathbf{P}_f - \mathbf{P}_{\tilde{f}} \mathbf{P}_{\tilde{f}_L}^{-1} \mathbf{P}_{f_L})^{-1} \Delta \mathbf{x}_i, \quad (18b)$$

or

$$\mathbf{b}_i = \mathbf{P}_f^{-1} (\mathbf{I}_{N+1} + \mathbf{P}_{\tilde{f}} (\mathbf{P}_{\tilde{f}_L} - \mathbf{P}_{f_L} \mathbf{P}_f^{-1} \mathbf{P}_{\tilde{f}})^{-1} \mathbf{P}_{f_L} \mathbf{P}_f^{-1}) \Delta \mathbf{x}_i, \quad (19a)$$

$$\tilde{\mathbf{b}}_i = -(\mathbf{P}_{\tilde{f}_L} - \mathbf{P}_{f_L} \mathbf{P}_f^{-1} \mathbf{P}_{\tilde{f}})^{-1} \mathbf{P}_{f_L} \mathbf{P}_f^{-1} \Delta \mathbf{x}_i. \quad (19b)$$

Additionally, when the rank of the coefficient matrix is smaller than  $2(N+1)$  and equals to that of the augmented matrix, there will be infinite solutions in (15). In this case, the inverse of the coefficient matrix in (17) is changed to the Moore-Penrose pseudo-inverse for a minimum norm solution.

Finally, from Fig. 1, (2), (14), and (17), the low-interference  $N$ -continuous symbol  $\bar{\mathbf{x}}_i$  is expressed as in (20), where  $M_s$  is the number of the OFDM symbols, and  $\mathbf{d}_{-1}$  is initialized as a zero vector  $\mathbf{d}_{-1} = \mathbf{0}_{K \times 1}$ .

#### IV. SIMULATION RESULTS

In this section, we show our performance results characterizing the continuity-enhanced basis signal aided low-interference  $N$ -continuous scheme employing the simulation parameters shown in Table I. For comparison, the performance of original OFDM and NC-OFDM is also considered. To demonstrate the performance of sidelobe suppression, the power spectrum density (PSD) is evaluated by Welch's averaged periodogram method with a 2048-sample Hanning window and 512-sample overlap after observing  $10^5$  symbols. To visualize the effect of the interference to the system transmission performance, we plot the BER in the multipath Rayleigh fading channel.

Fig. 2 shows the sidelobe suppression performance among original OFDM, conventional NC-OFDM [1], and the proposed scheme, where we set  $N=0,2,4,6$  and  $L=72,144,1024$ .

TABLE I  
SIMULATION PARAMETERS

Parameters	Values
Constellation modulation	16QAM
Number of subcarriers ( $K$ )	256
Subcarrier index set ( $\mathcal{K}$ )	$\{-128, -127, \dots, 127\}$
OFDM symbol duration	1/15 ms
Frequency interval ( $\Delta f$ )	15 KHz
Sampling interval ( $T_{\text{samp}}$ )	32.55 ns
Carrier frequency	2 GHz
Maximum Doppler shift ( $f_D$ )	111.11 Hz
Length of CP in OFDM ( $M_{cp}$ )	144

It can be seen that when the  $N$  is big, the NC-OFDM and the proposed scheme have a significant reduction of the out-of-band emission compared to OFDM. More importantly, by increasing the  $L$ , our low-interference scheme becomes capable of approaching the performance of the NC-OFDM. To specify this case, in Table II, we further calculate all curves in Fig. 2 in terms of adjacent channel leakage power ratio (ACLR), which is defined as the ratio of the average power in the band B0 to the average power out of the band B0 [12], where ACLR1 and ACLR2 is associated with the band B1 ( $B1 \neq B0$ ) close to B0 and the band B2 ( $B2 \neq B0$ ) far from B0, respectively. The results are calculated upon the bandwidth of B0 equal to that of B1 and equal to that of B2. It can be observed that the ACLR of the proposed scheme is close to that of NC-OFDM for a small  $L$ , such as  $L=72$ , namely the  $N$ -continuity is well guaranteed by the proposed scheme with the short-length smooth signal.

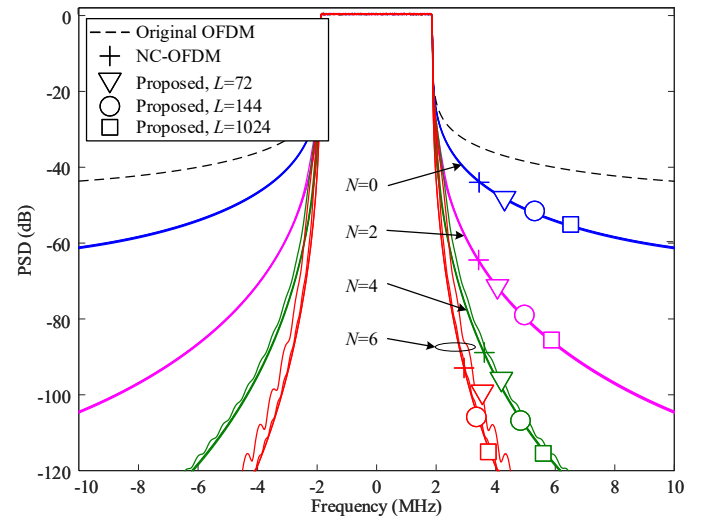


Fig. 2. PSD comparison of original OFDM, NC-OFDM, and the low-interference scheme with different  $N$ s and different  $L$ s.

TABLE II  
NUMERICAL RESULTS OF ACLR CORRESPONDING TO FIG. 2

Scheme		ACLR1 (dB)	ACLR2 (dB)
OFDM		34	42
NC-OFDM	$N=0$	40	58
	$N=2$	51	93
	$N=4$	61	126
	$N=6$	70	149
Proposed	$N=0$	$L=72$	40
		$L=144$	40
		$L=1024$	40
	$N=2$	$L=72$	48
		$L=144$	51
		$L=1024$	51
	$N=4$	$L=72$	50
		$L=144$	58
		$L=1024$	60
	$N=6$	$L=72$	52
		$L=144$	62
		$L=1024$	70

Fig. 3 shows the BER performance of the proposed scheme in conjunction with the channel tap delay [0, 30, 150, 310, 370, 710, 1090, 1730, 2510] ns and the channel relative power [0, -1.5, -1.4, -3.6, -0.6, -9.1, -7, -12, -16.9] dB [13], as well as that of the original OFDM and the NC-OFDM. Furthermore, the perfect channel information is known at the receiver and the zero-forcing channel equalization is adopted. The curves of the proposed scheme exhibit promising BER results, which are close to that of the original OFDM, while the NC-OFDM receiver exhibits worse performance for a big  $N$ , such as  $N=6$ . Even if a recovery for interference cancellation with 8 iterations [1] is considered, the floor emerges at  $E_b/N_0=35$ dB. It can be also inferred that the proposed scheme's performance in this simulation can be unaffected by the smooth signal. This owing to the fact that the proposed scheme is capable of adaptively reducing the length of the smooth signal so short that the channel-delayed smooth signal cannot interfere the useful signal.

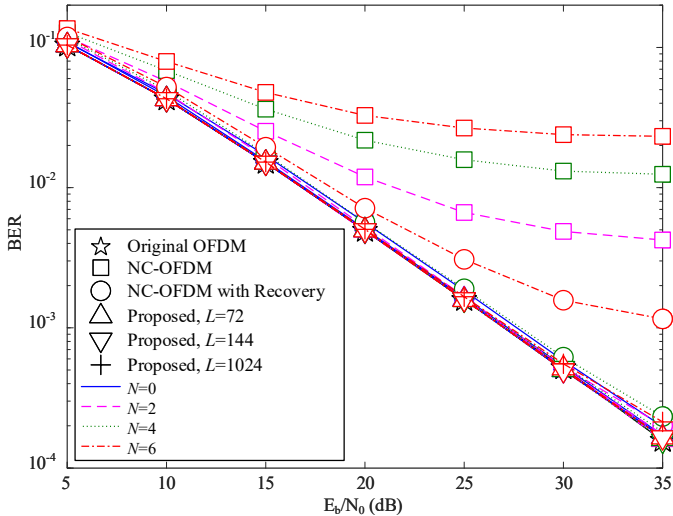


Fig. 3. BERs of original OFDM, the NC-OFDM, and the proposed scheme with different  $N$ s and different  $L$ s.

Additionally, we compute the number of complex multiplications of the proposed scheme by presetting

$[Q_f \ Q_{\tilde{f}}] \begin{bmatrix} P_f & P_{\tilde{f}} \\ P_{fL} & P_{\tilde{f}L} \end{bmatrix}^{-1}$  as an  $L \times (2N + 2)$  matrix, which is  $(N + 1)(L + 2K)$ . As shown above, since the good sidelobe suppression performance and BER performance can be achieved for a small  $L$ , such as  $L=72$  far smaller value than  $K=256$ , the complexity of the proposed scheme is comparable to that of the low-complexity schemes in [8] and [9], which is proportional to  $(N + 1)K$ . Furthermore, except the parameter matrices and the current input data  $x_i$ , the proposed scheme requires  $N+1$  numbers of memories for storing  $\Delta x_i$ , since  $N \ll K$ , which are far smaller than that in [8] storing  $K$  elements in  $x_{i-1}$  and slightly bigger than that in [9] without the storage for the previous symbol.

## V. CONCLUSION

In this letter, we proposed a low-interference two linear combination representations aided  $N$ -continuous OFDM designed for the sidelobe suppression, upon enhancing the continuities of the basis signals and their high-order derivatives. Our simulation results revealed that the BER of the proposed scheme can be reduced close to that of the original OFDM by a short-length smooth signal, while keeping the computation complexity comparable to other low-complexity NC-OFDM schemes and achieving the close sidelobe suppression performance to the conventional NC-OFDM.

## REFERENCES

- [1] J. van de Beek and F. Berggren, "N-continuous OFDM," *IEEE Commun. Lett.*, vol. 13, no. 1, pp. 1-3, Jan. 2009.
- [2] J. van de Beek and F. Berggren, "Out-of-band power suppression in OFDM," *IEEE Commun. Lett.*, vol. 12, no. 9, pp. 609-611, Sep. 2008.
- [3] M. Ohta, A. Iwase, and K. Yamashita, "Improvement of the error characteristics of an  $N$ -continuous OFDM system with low data channels by SLM," in *Proc. IEEE Int. Conf. Commun. (ICC)*, Kyoto, Japan, Jun. 2011, pp. 1-5.
- [4] M. Ohta, M. Okuno, and K. Yamashita, "Receiver iteration reduction of an  $N$ -continuous OFDM system with cancellation tones," in *Proc. IEEE Glob. Telecommun. Conf. (GLOBECOM)*, Kathmandu, Nepal, Dec. 2011, pp. 1-5.
- [5] H. Kawasaki, M. Ohta, and K. Yamashita, "Extension of  $N$ -continuous OFDM precoder matrix for improving error rate," *IEEE Commun. Lett.*, vol. 19, no. 2, pp. 283-286, Feb. 2015.
- [6] M. Mohamad, R. Nilsson, and J. van de Beek, "Minimum-EVM  $N$ -continuous OFDM," in *Proc. IEEE Int. Conf. Commun. (ICC)*, Kuala Lumpur, Malaysia, May 2016, pp. 1-5.
- [7] R.-A. Pitaval, B. M. Popović, and J. van de Beek, "N-continuous SC-FDMA and its polarized transmission and reception," *IEEE Trans. Commun.*, vol. 65, no. 11, pp. 4911-4925, Nov. 2017.
- [8] H. Kawasaki, M. Ohta, and K. Yamashita, "N-continuous symbol padding OFDM for sidelobe suppression," in *Proc. IEEE Int. Conf. Commun. (ICC)*, Sydney, Australia, Jun. 2014, pp. 5890-5895.
- [9] T. Taheri, R. Nilsson, and J. van de Beek, "Quasi-cyclic symbol extensions for shaping the OFDM spectrum," *IEEE Trans. Wireless Commun.*, vol. 17, no. 10, pp. 7054-7066, Oct. 2018.
- [10] P. Wei, L. Dan, Y. Xiao, and S. Li, "A low-complexity time-domain signal processing algorithm for  $N$ -continuous OFDM," in *Proc. IEEE Int. Conf. Commun. (ICC)*, Budapest, Hungary, Jun. 2013, pp. 5754-5758.
- [11] P. Wei, L. Dan, Y. Xiao, W. Xiang, and S. Li, "Time-domain  $N$ -continuous OFDM: System architecture and performance analysis," *IEEE Trans. Veh. Technol.*, vol. 66, no. 3, pp. 2394-2407, Mar. 2017.
- [12] *E-UTRA RF system scenarios Radio Frequency (RF) system scenarios (Release 15)*, 3GPP TR 36.942, v15.0.0, Jun. 2018. [Online]. Available: <http://www.3gpp.org/>.
- [13] *E-UTRA Base Station (BS) radio transmission and reception (Release 15)*, 3GPP TS 36.104, v15.4.0, Sep. 2018. [Online]. Available: <http://www.3gpp.org/>.